*Research sponsored by the U.S. Air Force Office of Scientific Research, Office of Aerospace Research, under Grant No. AFOSR68-1507.

[1]H. Hellmann, *Einfuhrung in die Quantenchemie* (Franz Deuticke, Leipzig, 1937), p. 285.

[2]R. P. Feynman, Phys. Rev. 56, 340 (1939).

[3]If the core electrons are tightly bound, the theorem can be stated in terms of the ion cores and valence electron charge distribution.

[4]G. H. Wannier, C. Misner, and G. Schay, Jr., Phys. Rev. 185, 983 (1969).

[5]L. Kleinman, Phys. Rev. B 1, 4189 (1970).

[6]G. H. Wannier and G. Meissner, Phys. Rev. B 3, 1240 (1971).

[7]We neglect edges where surface planes intersect.

[8]The fact that the x and y surfaces are corrugated does not effect the z component of force except near the x and y surfaces, but since the sign of this component of force changes as n_{jz} changes by increments of 0.5, it yields a negligible contribution to the pressure, down by a factor of $N^{-1/3}$ from the terms we are considering.

[9]Equation (5) is conditionally convergent, and one may obtain any value one wishes for P_{internal} by varying either the shape or the location of the center of the unit cells. However, for a finite crystal the pressure given by Eq. (4) is unique, and any change in the definition of the unit cell gives a corresponding change in the definition of the surface charge, so that P remains unchanged.

[10]Note that $\delta\rho$ represents the surface charge-density anomaly due to nuclei and electrons *of the metal* in their free response to whatever external forces act on them; if $\delta\rho$ included the charges producing these external forces Eq. (4) would yield zero pressure for any state of compression (because the total force on every ion always vanishes). Because we use the equilibrium lattice constant, we expect the charge distribution of the metal to be such that Eq. (4) yields zero pressure.

[11]A factor of 2 due to the two z surfaces cancels the factor of $\frac{1}{2}$.

PHYSICAL REVIEW B VOLUME 3, NUMBER 10 15 MAY 1971

Study of the Line Shapes for the Radio-Frequency Size Effect in Cadmium †

D. A. Boudreau*‡ and R. G. Goodrich
Department of Physics and Astronomy, Louisiana State University, Baton Rouge, Louisiana 70803
(Received 3 August 1971)

The behavior of the line shapes of the radio-frequency size effect has been observed in cadmium both below and in the vicinity of the surface-impedance singularities as a function of surface condition and temperature. It is shown that recent theoretical line-shape calculations based on phenomenological parameters give quantitative and qualitative agreement with experiment, and on the basis of this, inferences on the role of surface scattering in measurements of the radio-frequency surface impedance are outlined. Comments concerning the implications of the present results on past measurements are given.

I. INTRODUCTION

In the past several years, the radio-frequency size effect (RFSE)[1,2] has become an important and widely used method for investigating the Fermi surfaces (FS) of high-purity metals. This technique involves the measurement of the radio-frequency (rf) surface impedance of a thin slab of a high-purity metal as a function of the dc magnetic field applied in the plane of the slab. At magnetic field strengths such that a large number of electronic orbits just span the sample thickness, a discontinuity in the surface impedance is observed. Through the use of the Lorentz equation, one can then relate real space-orbit dimensions to corresponding FS dimensions in k space in order to extract an extremal caliper of the FS. The necessity of interpreting the various line shapes which occur has been inherent in these studies. In particular, which point of the observed singularity corresponds to the actual FS caliper has been a central problem. In this pursuit, theoretical solutions of the boundary value problem have been attempted under various assumptions to try to bring into focus the mechanisms involved in selecting the particular electron orbits which give rise to the observed signals. In lieu of a definitive theoretical treatment, some investigators have exploited an observed frequency dependence of the line shapes by using extrapolation methods to obtain caliper values, while others have relied upon the implications of the existing theory, supported by some qualitative agreement found in its general ability to produce a reasonable facsimile of the observed RFSE singularities. Notwithstanding the difficulty in ascribing relative accuracy[3-5] to these two techniques, there is yet another problem involved in that the line shape for a given caliper may vary drastically under seemingly identical experimental conditions.[6,7] Furthermore, although not central to the issue of caliper point assignment, there remains an associated question concerning the magnetic field dependence of the surface impedance at fields well below that at which the RFSE singularity occurs. The present investigation was made

in an effort to resolve some of the apparent discrepancies observed in the line shapes occurring in high-purity cadmium metal under RFSE conditions in an attempt to define more clearly the general aspects of the over-all rf surface-impedance dependence upon applied magnetic field within the bounds of available theory.

The first theoretical treatment of line shapes was by Kaner and Fal'ko (KF).[8] In their approach, KF consider the particular case of unilateral excitation in which the applied rf electric field is present only on one face of the sample slab. The electric field distribution in the metal was calculated using an exponential-decay approximation under the assumptions of a spherical FS and completely diffuse scattering for surface trajectories. Surface trajectories are those electronic orbits which at some time along their trajectory collide with a surface, as opposed to bulk trajectories which never intersect the metal surface. The results of the KF theory gave some qualitative agreement with the line shape reported in potassium by Wagner and Koch (WK)[6,9]; however, the extent of the differences which may arise for a given RFSE line on samples with different mean free paths was pointed out by Peercy *et al.*[7] in analyzing their data on potassium. The line shape of the latter workers shows little resemblance to that in Refs. 6 and 9 even though the two experiments were performed with essentially equivalent experimental apparatus. More recently, Tsoi and Gantmakher (TG)[10] have reported observing line-shape variations in K as a function of both mean free path and sample thickness. The failure of the KF theory to resolve such differences constitutes a serious limitation on its reliability.

Recently, Juras[11] has obtained numerical solutions to the problem from which line shapes for a variety of experimental conditions may be calculated including the case of bilateral antisymmetric excitation in which the rf electric field is applied in opposite directions on either side of the sample. In two successive papers,[12,13] he proposes the possibility that surface scattering may play a significant role in contributing to the over-all surface impedance and explores this by extensive numerical calculations. The calculations are carried out in terms of a specularity function $S(\theta)$ and an ineffectiveness parameter η. These parameters describe, respectively, the probability of specular scattering as a function of incident angle θ for surface trajectories and the ratio of mean free paths of surface trajectories to bulk trajectories. Though phenomenological in content and microscopically incomplete, the model nevertheless apparently succeeds in resolving such differences in line shape as those observed in potassium, as well as pointing out further disparities in line shapes which may be expected within the bounds of the theory.

In Secs. II–IV, the technique used for the measurements in Cd is described, followed by a discussion of the results in the light of the theory. Finally, some comments on the implications of the present results on past measurements are made.

II. EXPERIMENTAL METHODS

Cadmium was selected for this study for two reasons: The sample preparation is relatively easy and the FS of cadmium is well known.[14] Cadmium single-crystal slabs approximately 1 mm thick were cut with an acid saw from a bar of 99.9999%-pure Cd. These rough-cut slabs were aligned by Laue back-reflection photographs so that the surface normal was along the desired axis to within 0.5°. They were then planed flat on one side by spark erosion without removal from the x-ray goniometer. The slab was then removed from the goniometer and the goniometer table was planed flat. The slab was placed planed-side down on the goniometer table and attached by conductive silver aerosol spray, care being taken not to allow any spray to run beneath the slab. Then the opposite side was planed parallel to the first with a final slab thickness of approximately 0.5 mm. The thin layer of spark-damaged surface was removed by etching the slab for about 30 sec in a bath of 70% nitric acid at 0 °C. Finally, samples 5×5 mm were cut from the slabs to remove the edges which became rounded during the etching process. The final sample surfaces ranged in condition from very smooth to extremely rough. Qualitative comparisons were done on a scanning electron microscope with magnifications up to 1000×.

The measuring apparatus has been described pre-

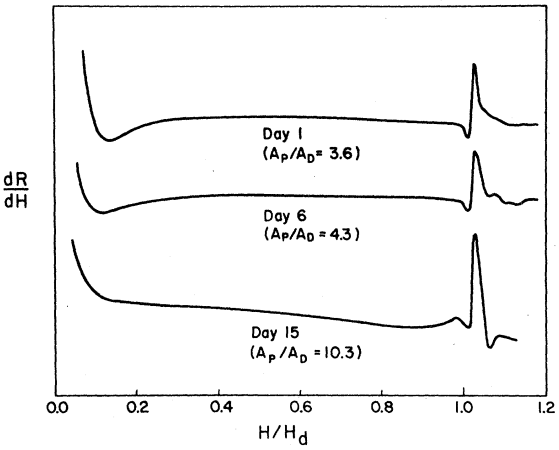

FIG. 1. Recorder tracings on a typical Cd sample over a period of 15 days giving dR/dH in arbitrary units vs H/H_d. Ratio of the amplitude of the first peak to the amplitude of the first dip is shown for each. Data were taken at 1.2 °K with $\hat{n} \| [11\bar{2}0]$, $\vec{H} \| [10\bar{1}0]$, $f = 12.0$ MHz, and $H_d = 85.1$ G.

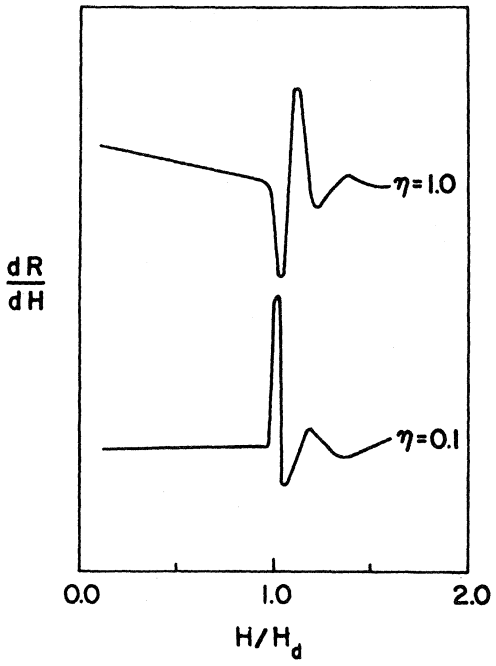

FIG. 2. Theoretical curves taken from Ref. 13 giving the expected change in dR/dH vs H/H_d as a function of the ineffectiveness parameter η for bilateral antisymmetric excitation.

viously by Steenhaut and Goodrich.[15] A digital rf frequency counter was added to the detection circuitry for studies of the frequency dependence. This apparatus allows both the first and second harmonic of the impressed modulation frequency to be detected. The sample was placed in a preformed coil wound on a Formica form of dimensions slightly larger than the sample. In this way, reasonable uniformity in the filling factor of the coil could be maintained through repeated use of the same coil and sample size. The coil formed the inductive element in a modified version of the high-level marginal oscillator providing bilateral antisymmetric excitation of the sample. The sample was immersed in a liquid-helium bath, the temperature of which was controlled by pumping through a diaphragm-type pressure regulator.

III. RESULTS AND DISCUSSION

All of the RFSE line shapes which will be discussed arise from the third-band electron sheet (lens) of the Cd FS. Since this portion of the FS comprises one-half of the carriers in Cd and there is only one band of extremal orbits on it for any orientation of the field, it dominates the surface impedance in these measurements. In Fig. 1, recorder tracings of the derivative of the real part of the surface impedance, dR/dH, as a function of

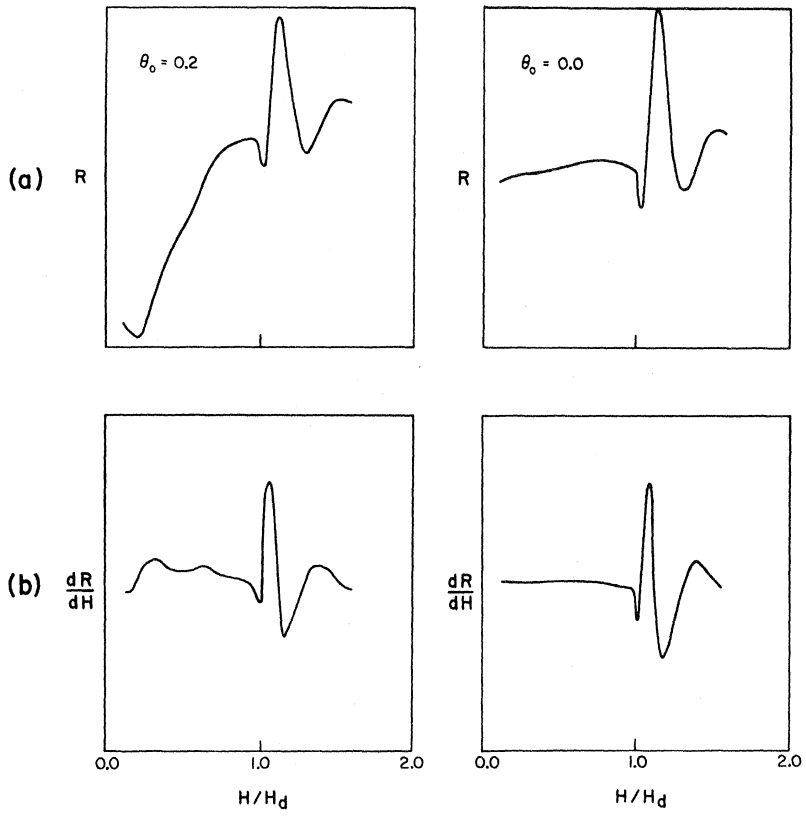

FIG. 3. (a) Theoretical curves taken from Ref. 12 giving the predicted R-vs-H dependence as a function of "critical angle" θ_0 for bilateral antisymmetric excitation. (b) Derivatives of the curves in (a).

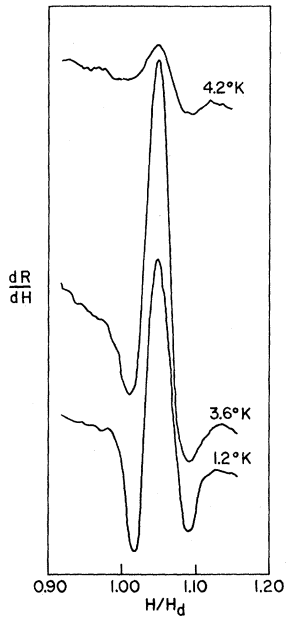

FIG. 4. Recorder tracings of the RFSE arising from the lens orbit in Cd in the configuration $\hat{n} \parallel [11\bar{2}0]$, $\vec{H} \parallel [0001]$ as a function of temperature. Curve at 1.2 °K is reduced by a factor of 4 in gain. Oscillator frequency was 5.2 MHz and $H_d = 202$ G.

applied field are shown. These data were collected on a typical sample over a period of 15 days. The original condition of the sample surfaces was shiny with a typical lemon-peel texture. Once placed in the Dewar, it was not removed for the duration, although recycling to room temperature occurred on several occasions. The striking change in line shape for all values of field from $H/H_d = 0$ to $H/H_d = 1.1$ from day 1 to day 15 under uniform experimental conditions clearly indicates the existence of underlying factors involved in RFSE line formation. Here H_d corresponds to the field at which the orbit exactly spans the sample thickness. In fact, upon removal of the sample on day 15, surface deterioration was clearly visible, implying that the contrasting line shapes were reflecting a change in surface character. The theoretical curves from the Juras theory for the expected change in dR/dH as a function of the ineffectiveness parameter η are shown in Fig. 2. As η decreases, the predicted line-shape behavior is that of increasing peak-to-dip-amplitude ratio, culminating in the loss of the initial dip. The measured change in the peak-to-dip-amplitude ratio A_P/A_D, listed adjacent to each of the corresponding experimental curves in Fig. 1, shows that this behavior is observed here, as seen previously in the data on K of Refs. 6–9 and discussed in Ref. 13.

A further aspect of the experimental curves of Fig. 1 is the change in the nature of the RFSE lines below $H/H_d = 1$. The distinct roll over in dR/dH at $H/H_d \approx 0.2$, seen in the two upper curves, gives way to a monotonically decreasing line in the lower trace. This behavior at fields below $H/H_d = 1$ bears strong resemblance to the curves predicted by the Juras model as a function of the specularity function $S(\theta)$ and the additional device of a "critical angle" θ_0.[12] The predicted R-vs-H dependence as a function of θ_0 for two values, $\theta_0 = 0.2$ and $\frac{1}{2}\pi$ rad taken from Ref. 12, is shown in Fig. 3(a) and the corresponding derivatives in Fig. 3(b). Basically, $S(\theta)$ describes the nature of surface scattering as a function of incident angle θ through the definition

$S(\theta) = 1$ completely specular,

$S(\theta) = 0$ completely diffuse,

and $0 \leq S(\theta) \leq 1$ is used parametrically. The incorporation of a "critical-angle" parameter θ_0 allows the additional degree of freedom for a possible change over the conditions of dominantly specular scattering for $\theta < \theta_0$ to that of dominantly diffuse scattering for $\theta > \theta_0$. By definition, $S(\theta_0 = 0) = 1$ and $S(\theta_0 = \frac{1}{2}\pi) = 0$ for all θ. Comparing Figs. 1 and 3(b) clearly shows the similarity for $H/H_d < 1$ between the top two experimental curves and the predicted curve for $\theta_0 = 0.2$ rad. Further, the predicted curve for completely diffuse scattering, $\theta_0 = \frac{1}{2}\pi$, shows the same monotonic decrease for $H/H_d < 1$ as the experimental curve associated with the deteriorated sample surface.

Another observed line-shape variation which seems to be associated with the functional depen-

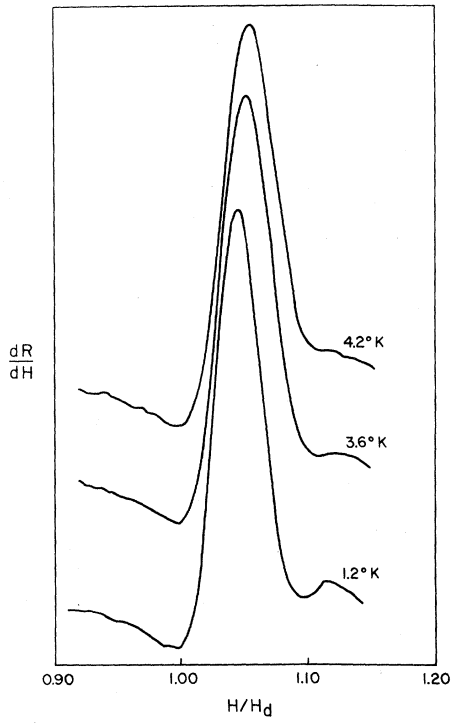

FIG. 5. Recorder tracings of the RFSE arising from the lens orbit in Cd in the configuration $\hat{n} \parallel [11\bar{2}0]$, $\vec{H} \parallel [10\bar{1}0]$ as a function of temperature. Curves at 3.6 and 1.2 °K are reduced by factors of 2 and 20, respectively. Oscillator frequency was 5.2 MHz and $H_d = 72.5$ G.

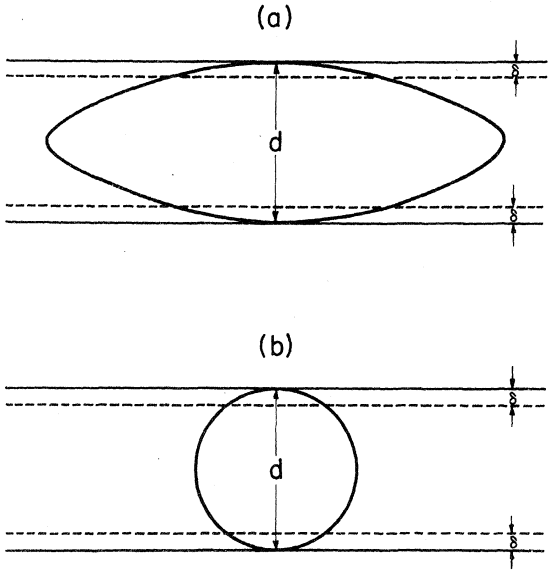

FIG. 6. (a) Real-space trajectories of the Cd lens extremal orbits in the configuration $\hat{n} \| [11\bar{2}0]$, $\vec{H} \| [10\bar{1}0]$. (b) Real-space trajectories of the Cd lens extremal orbits in the configuration $\hat{n} \| [11\bar{2}0]$, $\vec{H} \| [0001]$.

dence of mean free path upon temperature is shown in the experimental tracings of Figs. 4 and 5. The data were taken from two samples having identical surfaces as observed under a microscope. The real-space lens trajectories giving rise to the two lines are illustrated in Fig. 6. The salient point here is the significant change in line shape exhibited in Fig. 4, particularly the magnitude of the first dip, as opposed to the relatively lesser changes in Fig. 5. The change in mean free path as a function of temperature can be expressed through the use of the parameter κ defined as the ratio of bulk mean free path to sample thickness l/d. Since the bulk mean free path in these samples increases from ≈ 1 to ≈ 4 mm as the temperature is reduced from 4.2 to 1.2 °K, [16] this corresponds to a change from $\kappa = 2$ to $\kappa = 8$ for the above data. In Figs. 7(a) and 7(b), the theoretically predicted behavior of R vs H from the Juras model as a function of κ is shown for the cases of completely specular and completely diffuse surface scattering for $\kappa = 1$ and 4; Figs. 7(c) and 7(d) show the corresponding derivative curves. The similarities between experimental and theoretical curves for the two values of κ are quite evident. Along with the exaggerated changes predicted for the diffuse case, Fig. 7(d) also shows an expected line narrowing in the specular case as κ increases. It is to be noted that both of these calculated results are consistent with the experimental data of Figs. 4 and 5. Upon comparing the two different-type trajectories shown in Fig. 6, it is seen that trajectories in the samples with $\vec{H} \| [10\bar{1}0]$ and which exhibit a specular line shape have a much larger radius of curvature than the case where $\vec{H} \| [0001]$ and a diffuse line shape is observed. For those portions of the trajectories which lie entirely within the skin depth between collisions with the surface, the angle of incidence with the surface is much smaller with $\vec{H} \| [10\bar{1}0]$ than with $\vec{H} \| [0001]$. This result is consistent with the theoretically proposed angle-dependent specularity func-

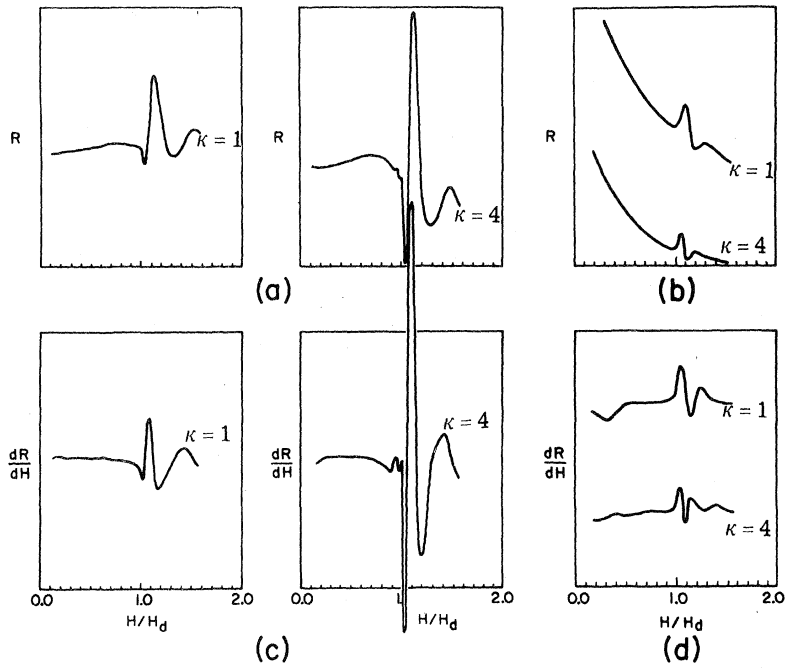

FIG. 7. Theoretical curves taken from Ref. 13 giving the expected change in behavior of R vs H as a function of κ for (a) completely diffuse and (b) completely specular surface scattering for bilateral antisymmetric excitation. Corresponding derivatives are shown in (c) and (d).

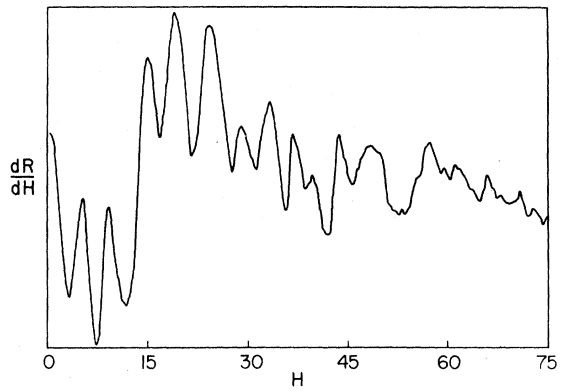

FIG. 8. Recorder tracing of dR/dH vs H for the low-field microwave surface impedance of a Cd sample in the configuration $\vec{H} \parallel [10\bar{1}0]$, $\vec{E} \parallel [0001]$ at 1.2°K using a 35-GHz spectrometer. Apparent surface-state transitions are clearly evident as high as $H = 70$ G.

tion in which the nature of the scattering is determined by the angle of incidence. An angular dependence for specular reflection has been previously noted by Koch and Murray in their microwave work on Ga and Sn.[17]

As mentioned previously, TG have reported line-shape variations in K as a function of both mean free path and sample thickness.[10] Although these in part were related to limiting-point trajectories in the tilted-field RFSE geometry (see, e.g., Ref. 2), the results of the measurements in the parallel-field geometry are pertinent to the present discussion. The change in line shape observed by TG in Ref. 10 as a function of mean free path in the tilted-field geometry appears to be similar in several respects to those reported here for the case of diffuse scattering, namely, a marked increase in the prominence of the first dip at the onset of the RFSE for a given sample thickness as the temperature is decreased. Moreover, the line-shape variations illustrated by TG as a function of sample thickness in the standard geometry bear evident similarities to the κ-dependent variations reported here for diffuse scattering.

Finally, in an effort to explore further the implication that surface scattering may contribute significantly to the RFSE line shape, low-field microwave surface-impedance measurements were made on a Cd sample ($\hat{n} \parallel [11\bar{2}0]$) with a surface identical to those previously described. The resulting recorder tracing of $\partial R/\partial H$ vs H showing several series of peaks for $\vec{H} \parallel [10\bar{1}0]$, $\vec{E} \parallel [0001]$ at 1.2°K, using a 35-GHz spectrometer, is shown in Fig. 8. Such oscillations in the low-field microwave surface impedance have been explained theoretically by Nee and Prange (NP)[18] in terms of transitions between quantum surface states,[19] the existence of which is dependent upon the specular nature of surface scattering for grazing incidence trajectories giving rise to "skipping" orbits.[17] Although analysis of these results is incomplete at present, their observation alone is satisfying. The appearance of peaks as high in field as 70 G in the one case illustrated in Fig. 8 for $\hat{n} \parallel [11\bar{2}0]$, $\vec{E} \parallel [0001]$ gives ample evidence within the bounds of the NP theory that skipping orbits can be sustained in these samples as high in field as $H/H_d = 1$ for the trajectories of the type illustrated in Fig. 6(a).

IV. CONCLUSION

The cataloged behavior of RFSE line shapes both below and in the vicinity of $H/H_d = 1$, presented here as a function of surface condition and temperature, shows good agreement with theory. The quantitative and qualitative similarities between the experimental and theoretical curves show that the character of the sample surface strongly affects the RFSE line shape in a way which is theoretically predictable through the use of a phenomenological model incorporating a specularity function $S(\theta)$ and an ineffectiveness parameter η. The proposed mechanism of "skipping-orbit" contributions to RFSE line shapes

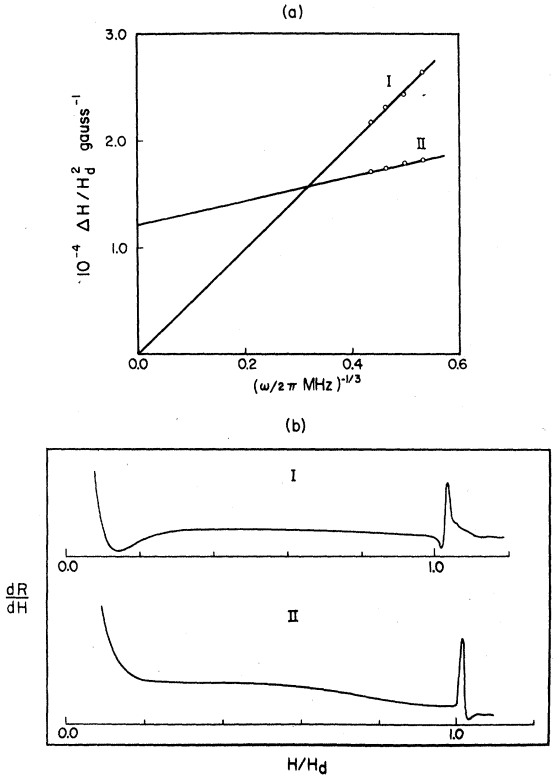

FIG. 9. (a) Dependence of linewidth on $(\omega/2\pi)^{-1/3}$ for two different Cd samples at 1.2°K. The linewidth ΔH is divided by the square of the critical field, constant for each curve. (b) Typical recorder tracings of dR/dH vs H for the two samples. Both traces were taken at 12.2 MHz.

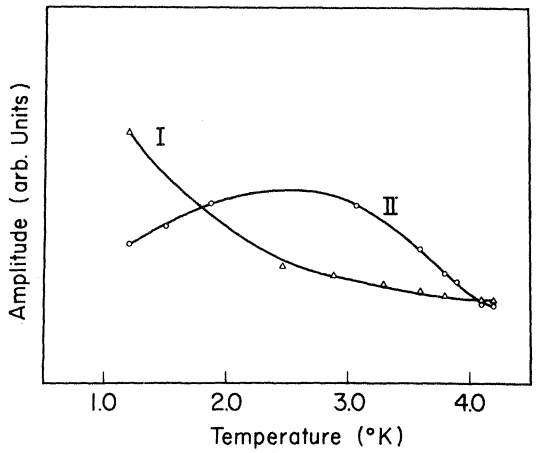

FIG. 10. Temperature dependence of the amplitudes of two RFSE lines in Cd, both of which arise from the lens orbits. Curve I is for the configuration $\hat{n} \| [11\bar{2}0]$, $\vec{H} \| [10\bar{1}0]$ and II is for $\hat{n} \| [11\bar{2}0]$, $\vec{H} \| [0001]$. Amplitudes, as defined in Sec. IV of the text, are normalized at 4.2 °K and plotted on a linear scale. Data were taken at 12.2 MHz.

is made plausible on the basis of the experiment-theory agreement coupled with the additional low-field microwave surface-impedance measurement data which show the existence of quantum surface states, hence skipping orbits, at fields approaching $H/H_d = 1$ in the cases reported here.

In view of the results obtained from the temperature- and surface-condition studies, it appears that the theory gives a reliable choice for assigning critical-field values to RFSE singularities, namely, the field value at which the first maximum rate of deviation in R is observed.[12] The equity of this assignment is further borne out by the successful comparison of calipered FS cross sections in Cd, Zn, and Tl with the corresponding de Haas–van Alphen data. In this regard, it is noted here that in the course of this investigation, a deviation from the generally expected $\Delta H \propto \omega^{-1/3}$ relationship[1,2] was observed. This deviation was also noted previously by Haberland and Shiffman (HS)[20] from their measurements on Ga. Plots of $\Delta H/H_d^2$ vs $(\omega/2\pi)^{-1/3}$ for two samples are shown in Fig. 9(a), and their over-all dR/dH field dependence in Fig. 9(b) for one of the frequency points. Based on the previous discussion in which curves of the character of Fig. 9(b) curve I may be classified as specular types and those of Fig. 9(b) curve II as diffuse types, there is evidence that surface scattering affects the frequency dependence of the linewidth in such a way as to alter the $\Delta H \propto \omega^{-1/3}$ relationship. Recently, this relationship has been used to extract calipers from RFSE data.[5] The present data indicate, however, that caliper values obtained by this type of extrapolation may be dependent on sample surface conditions and orbit geometry.

As a final note, Fig. 10 is a plot of the RFSE line amplitude as a function of temperature for the data from which the curves of Figs. 4 and 5 were taken. Here, the amplitude is defined as the difference between values of dR/dH taken at the first two prominent extrema of the RFSE line. The resulting curves graphically display the predicted behavior of line-shape dependence upon κ and surface scattering, namely, that diffuse types are to show dominant increase in amplitude of the first dip over the rest of the line while specular types are to show little change except for a possible decrease in the amplitude of the first dip. These curves are similar to those reported by HS[20] for gallium. Their analysis, however, was based on a different model from which they extracted the temperature dependence of the mean collision time τ and the cyclotron frequency of the electronic orbits on different FS sheets. Their model is based on the idea that the phase shift of the rf field between successive orbits of electrons which traverse both skin layers at least once produces a change in the total current in each skin layer. According to this model, different FS sheets having different mean collision times would suffer different losses as a function of temperature and this mechanism would produce the results reported. In the cases shown in Fig. 10 for Cd, both curves are due to the *same* FS sheet, in which case the HS model breaks down. The effect of the phase-shift mechanism upon which their model is based is similar to that mentioned by Juras in which interference between currents produced by bulk trajectories and surface trajectories produce changes in line shape as a function of κ and surface scattering.

†Work performed under the auspices of the National Science Foundation under Grant No. GP-1108.

*Present address: Division of Mathematics and Science, Huntingdon College, Montgomery, Ala.

‡The financial assistance received from the Dr. Charles E. Coates Memorial Fund of the Louisiana State University Foundation, donated by George H. Coates, for the preparation of this manuscript is gratefully acknowledged.

[1]V. F. Gantmakher, Zh. Eksperim. i Teor. Fiz. 42, 1416 (1962); 43, 345 (1962); 44, 811 (1963) [Sov. Phys. JETP 15, 982 (1962); 16, 247 (1962); 17, 549 (1963)].

[2]For a review of RFSE, see, for example, V. F. Gantmakher, in *Progress in Low Temperature Physics*, edited by C. J. Gorter (North-Holland, Amsterdam, 1966), Vol. 5, p. 181 or W. M. Walsh, Jr., in *Solid State Physics*, edited by J. F. Cochran and R. R. Haering (Gordon and Breach, New York, 1968), Vol. 1, p. 173.

[3]V. V. Boiko, V. A. Gasparov, and I. G. Gverdtsiteli, Zh. Eksperim. i Teor. Fiz. 56, 489 (1969) [Sov. Phys. JETP 29, 267 (1969)].

[4]G. Leaver and A. Myers, Phil. Mag. 19, 465 (1969).

[5]J. R. Cleveland and J. L. Stanford, Phys. Rev. Let-

ters 24, 1482 (1970).
[6]J. F. Koch and T. K. Wagner, Phys. Rev. 151, 467 (1966).
[7]P. S. Peercy, W. M. Walsh, Jr., L. W. Rupp, Jr., and P. H. Schmidt, Phys. Rev. 171, 713 (1968).
[8]E. A. Kaner and V. L. Fal'ko, Zh. Eksperim. i Teor. Fiz. 49, 1895 (1965) [Sov. Phys. JETP 22, 1294 (1966)].
[9]T. K. Wagner and J. F. Koch, Phys. Rev. 165, 885 (1968).
[10]V. S. Tsoi and V. F. Gantmakher, Zh. Eksperim. i Teor. Fiz. 56, 1234 (1969) [Sov. Phys. JETP 29, 663 (1969)].
[11]G. E. Juras, Phys. Rev. 187, 784 (1969).
[12]G. E. Juras, Phys. Rev. Letters 24, 390 (1970).
[13]G. E. Juras, Phys. Rev. B 2, 2869 (1970).
[14]R. C. Jones, R. G. Goodrich, and L. M. Falicov, Phys. Rev. 174, 672 (1968).
[15]O. L. Steenhaut and R. G. Goodrich, Phys. Rev. B 1, 4511 (1970).
[16]C. G. Grenier, K. R. Efferson, and J. M. Reynolds, Phys. Rev. 143, 406 (1966).
[17]J. F. Koch and T. E. Murray, Phys. Rev. 186, 722 (1969).
[18]T. W. Nee and R. E. Prange, Phys. Letters 25A, 582 (1967).
[19]For a review, see J. F. Koch, in *Solid State Physics*, edited by J. F. Cochran and R. R. Haering (Gordon and Breach, New York, 1968), Vol. 1, p. 253.
[20]P. H. Haberland and C. A. Shiffman, Phys. Rev. Letters 19, 1337 (1967).

PHYSICAL REVIEW B VOLUME 3, NUMBER 10 15 MAY 1971

Self-Consistent Energy Bands of Cu via the $X_{\alpha\beta}$ Method*

A. M. Boring
University of California, Los Alamos Scientific Laboratory, Los Alamos, New Mexico 87544
(Received 18 January 1971)

The energy bands of Cu have been calculated self-consistently through use of the improved exchange approximation of Herman, Van Dyke, and Ortenburger (the so-called $X_{\alpha\beta}$ method). The resulting bands are compared with the self-consistent energy bands calculated by the X_α method with $\alpha = 1.00$, $\frac{5}{6}$, 0.721, and $\frac{2}{3}$. The X_α and $X_{\alpha\beta}$ energy-band widths (s-p, d) are compared with photoemission data. The differences between the energy-band calculations and the atomic calculations are described. A brief discussion is given of the role of the virial theorem and the variational principle.

I. INTRODUCTION

Since Herman[1] proposed the improved approximation ($X_{\alpha\beta}$) for the exchange operator, there have been several atomic calculations[2-4] incorporating it. Herman has shown[2] that the total energies of atoms calculated via Hartree-Fock (HF) theory using $X_{\alpha\beta}$ orbitals are in better agreement with HF total energies (determined from HF orbitals) than are HF total energies calculated from X_α orbitals. It has also been shown that the parameter β (with $\alpha = \frac{2}{3}$) in the $X_{\alpha\beta}$ method is less sensitive to atomic number (z) and the Latter potential shift in atomic systems than is the parameter α of the X_α scheme.[4] In this paper we present the results of a calculation for which the $X_{\alpha\beta}$ method was proposed, the energy-band structure of a crystal.

In Sec. II, a discussion is given of the statistical exchange methods (X_α and $X_{\alpha\beta}$), and the difference between $X_{\alpha\beta}$ calculations in atoms and in crystals is pointed out. In Sec. III, we give the results of a self-consistent calculation of the energy-band structure of Cu using the $X_{\alpha\beta}$ exchange approximation. In that section we also compare the results of this calculation with the self-consistent energy bands of Cu calculated by the X_α method for $\alpha = 1.00$, $\frac{5}{6}$, 0.721, and $\frac{2}{3}$. In Sec. IV the role of the virial theorem and the variational principle in these statistical exchange approximations is discussed.

II. METHOD

In the X_α method, the local one-electron exchange operator is written as

$$V_x^\alpha(r) = \alpha V_{xs}(r) ,$$

where

$$V_{xs}(r) = -6[3\pi/8\rho(r)]^{1/3}$$

is the Slater exchange,[5] and $\rho(r)$ is the electronic charge density of the system. In the X_α method, the constant α can be determined for a given atom by generating a set of orbitals $\{\Phi(\alpha)\}$ that minimizes[6] the Hartree-Fock total energy E^{HF}, i.e.,

$$\alpha_{\min} \rightarrow \{\Phi(\alpha_{\min})\} \rightarrow E^{\mathrm{HF}}[\Phi(\alpha_{\min})] ,$$

where $E^{\mathrm{HF}}[\Phi(\alpha_{\min})]$ is total HF energy calculated with X_α orbitals. Kmetko[7] has obtained in this manner a set of $\alpha_{\min}$'s for all the atoms in the Periodic Table. Since $\frac{2}{3}$ is considered to be the correct value of α for a nearly homogeneous electron gas,[8] deviations from this value may be con-